Table 3. Relationship between liver fibrosis stage, RTE image features and LFI

	HCV				p value	HBV				p value
	F1 (n = 179)	F2 (n = 98)	F3 (n = 62)	F4 (n = 75)		F1 (n = 69)	F2 (n = 12)	F3 (n = 16)	F4 (n = 31)	
RTE features										
MEAN	113.9 (107.2, 119.9)	109.6 (102.2, 115.1)	103.0 (94.8, 111.6)	93.4 (82.5, 105.0)	<0.0001	117.8 (107.4, 122.3)	119.0 (112.7, 121.8)	108.6 (103.1, 116.5)	101.4 (87.7, 109.7)	<0.0001
SD	52.3 (45.9, 58.7)	57.3 (50.6, 60.7)	59.6 (54.7, 63.4)	60.9 (57.6, 63.9)	<0.0001	49.1 (44.6, 56.9)	50.6 (44.6, 54.2)	57.3 (52.2, 61.5)	63.4 (56.9, 65.1)	<0.0001
AREA	14.2 (7.6, 20.8)	19.1 (11.8, 27.2)	25.2 (16.3, 33.7)	34.5 (22.5, 44.2)	<0.0001	11.2 (6.2, 19.2)	11.3 (6.2, 16.2)	20.6 (13.5, 27.7)	29.0 (19.8, 39.2)	<0.0001
COM	20.3 (18.5, 24.1)	22.8 (19.8, 26.2)	25.2 (21.3, 29.9)	31.3 (24.6, 40.2)	<0.0001	20.1 (18.5, 25.8)	20.7 (19.6, 21.8)	24.5 (21.3, 30.2)	28.9 (23.6, 34.5)	<0.0001
ASM	0.00025 (0.00019, 0.00035)	0.00020 (0.00017, 0.00032)	0.000212 (0.000178, 0.000315)	0.000294 (0.000190, 0.000453)	0.983	0.000209 (0.000183, 0.000268)	0.000196 (0.000170, 0.000220)	0.000177 (0.000175, 0.000188)	0.000213 (0.000177, 0.000285)	0.159
CON	229.6 (173.4, 268.6)	250.0 (206.9, 309.0)	261.2 (213.5, 324.0)	266.7 (233.8, 320.7)	<0.0001	221.7 (18.08, 285.2)	239.1 (198.4, 283.7)	272.2 (250.7, 279.0)	294.1 (249.1, 372.2)	<0.0001
COR	0.958 (0.947, 0.965)	0.958 (0.950, 0.966)	0.957 (0.950, 0.967)	0.962 (0.951, 0.966)	0.117	0.953 (0.944, 0.959)	0.946 (0.943, 0.955)	0.956 (0.947, 0.961)	0.954 (0.945, 0.968)	0.139
ENT	3.83 (3.76, 3.87)	3.85 (3.80, 3.89)	3.86 (3.81, 3.89)	3.84 (3.76, 3.88)	0.052	3.81 (3.74, 3.86)	3.80 (3.77, 3.86)	3.86 (3.84, 3.88)	3.84 (3.80, 3.89)	0.024
IDM	0.110 (0.095, 0.122)	0.101 (0.091, 0.117)	0.096 (0.091, 0.118)	0.108 (0.093, 0.122)	0.154	0.100 (0.091, 0.111)	0.092 (0.088, 0.100)	0.092 (0.089, 0.095)	0.100 (0.087, 0.106)	0.147
SKEW	0.199 (0.071, 0.300)	0.253 (0.122, 0.361)	0.332 (0.178, 0.461)	0.429 (0.321, 0.679)	<0.0001	0.116 (–0.517, 0.260)	0.124 (0.025, 0.219)	0.236 (0.178, 0.289)	0.376 (0.213, 0.540)	<0.0001
KURT	2.38 (2.24, 2.57)	2.34 (2.22, 2.48)	2.29 (2.20, 2.40)	2.34 (2.23, 2.64)	0.334	2.49 (2.31, 2.68)	2.48 (2.31, 2.63)	2.33 (2.29, 2.43)	2.33 (2.19, 2.47)	0.001
LFI	1.81 (1.41, 2.22)	2.10 (1.67, 2.56)	2.47 (1.97, 2.88)	2.97 (2.41, 3.45)	<0.0001	1.52 (1.16, 2.06)	1.61 (1.31, 1.84)	2.16 (1.66, 2.58)	2.66 (2.15, 3.13)	<0.0001

Values are presented as median (first quartile, third quartile). The p values were calculated with the Jonckheere-Terpstra trend test.

Oncology 2014;87(suppl 1):63–72
DOI: 10.1159/000368147

Table 4. Relationship between etiology, RTE image features and LFI

	F1		p value	F2		p value	F3		p value	F4		p value
	HCV (n = 179)	HBV (n = 69)		HCV (n = 98)	HBV (n = 12)		HCV (n = 62)	HBV (n = 16)		HCV (n = 75)	HBV (n = 31)	
RTE features												
MEAN	113.9 (107.2, 119.9)	117.8 (107.4, 122.3)	0.012	109.6 (102.2, 115.1)	119.0 (112.7, 121.8)	0.003	103.0 (94.8, 111.6)	108.6 (103.1, 116.5)	0.033	93.4 (82.5, 105.0)	101.4 (87.7, 109.7)	0.057
SD	52.3 (45.9, 58.7)	49.1 (44.6, 56.9)	0.091	57.3 (50.6, 60.7)	50.6 (44.6, 54.2)	0.006	59.6 (54.7, 63.4)	57.3 (52.2, 61.5)	0.162	60.9 (57.6, 63.9)	63.4 (56.9, 65.1)	0.395
AREA	14.2 (7.6, 20.8)	11.2 (6.2, 19.2)	0.121	19.1 (11.8, 27.2)	11.3 (6.2, 16.2)	0.010	25.2 (16.3, 33.7)	20.6 (13.5, 27.7)	0.055	34.5 (22.5, 44.2)	29.0 (19.8, 39.2)	0.109
COM	20.3 (18.5, 24.1)	20.1 (18.5, 25.8)	0.985	22.8 (19.8, 26.2)	20.7 (19.6, 21.8)	0.114	25.2 (21.3, 29.9)	24.5 (21.3, 30.2)	0.757	31.3 (24.6, 40.2)	28.9 (23.6, 34.5)	0.186
ASM	0.00025 (0.00019, 0.00035)	0.000209 (0.000183, 0.000268)	0.008	0.00020 (0.00017, 0.00032)	0.000196 (0.000170, 0.000220)	0.242	0.000212 (0.000178, 0.000315)	0.000177 (0.000175, 0.000188)	0.006	0.000294 (0.000190, 0.000453)	0.000213 (0.000177, 0.000285)	0.027
CON	229.6 (173.4, 268.6)	221.7 (18.08, 285.2)	0.484	250.0 (206.9, 309.0)	239.1 (198.4, 283.7)	0.673	261.2 (213.5, 324.0)	272.2 (250.7, 279.0)	0.488	266.7 (233.8, 320.7)	294.1 (249.1, 372.2)	0.117
COR	0.958 (0.947, 0.965)	0.953 (0.944, 0.959)	0.003	0.958 (0.950, 0.966)	0.946 (0.943, 0.955)	0.004	0.957 (0.950, 0.967)	0.956 (0.947, 0.961)	0.245	0.962 (0.951, 0.966)	0.954 (0.945, 0.968)	0.534
ENT	3.83 (3.76, 3.87)	3.81 (3.74, 3.86)	0.238	3.85 (3.80, 3.89)	3.80 (3.77, 3.86)	0.153	3.86 (3.81, 3.89)	3.86 (3.84, 3.88)	0.990	3.84 (3.76, 3.88)	3.84 (3.80, 3.89)	0.629
IDM	0.110 (0.095, 0.122)	0.100 (0.091, 0.111)	0.002	0.101 (0.091, 0.117)	0.092 (0.088, 0.100)	0.071	0.096 (0.091, 0.118)	0.092 (0.089, 0.095)	0.026	0.108 (0.093, 0.122)	0.100 (0.087, 0.106)	0.019
SKEW	0.199 (0.071, 0.300)	0.116 (–0.517, 0.260)	0.015	0.253 (0.122, 0.361)	0.124 (0.025, 0.219)	0.039	0.332 (0.178, 0.461)	0.236 (0.178, 0.289)	0.065	0.429 (0.321, 0.679)	0.376 (0.213, 0.540)	0.083
KURT	2.38 (2.24, 2.57)	2.49 (2.31, 2.68)	0.005	2.34 (2.22, 2.48)	2.48 (2.31, 2.63)	0.034	2.29 (2.20, 2.40)	2.33 (2.29, 2.43)	0.158	2.34 (2.23, 2.64)	2.33 (2.19, 2.47)	0.200
LFI	1.81 (1.41, 2.22)	1.52 (1.16, 2.06)	0.029	2.10 (1.67, 2.56)	1.61 (1.31, 1.84)	0.010	2.47 (1.97, 2.88)	2.16 (1.66, 2.58)	0.051	2.97 (2.41, 3.45)	2.66 (2.15, 3.13)	0.042

Values are presented as median (first quartile, third quartile). The p values were calculated with the Mann-Whitney U test.

Table 5. Diagnostic performance of the LFI for liver fibrosis assessment

	HCV			HBV		
	F4	>F3	>F2	F4	>F3	>F2
AUROC	0.803	0.774	0.73	0.821	0.806	0.744
Cutoff	2.45	2.42	2.31	2.07	1.94	1.91
Positive predictive value	37.8	58.2	58.7	80.6	78.7	66.1
Negative predictive value	92.9	81.6	79.9	71.1	75.3	72.5
Intensity	74.7	65	79.3	47.2	64.9	67.2
Specificity	72.9	76.9	59.6	92	85.9	71.4
Accuracy	73.2	72.2	67.9	73.4	76.6	69.5

found to be significantly higher in HCV-infected patients at stages F1, F2, and F4 (F1: HCV = 181, HBV = 1.52, p = 0.029; F2: HCV = 2.10, HBV = 1.61, p = 0.010; F4: HCV = 2.97, HBV = 2.66, p = 0.042) and marginally higher in HCV-infected patients at stage F3 (HCV = 2.47, HBV = 2.16, p = 0.051) (table 4).

AUROC Analysis

The LFI cutoff values for each stage of fibrosis were calculated by AUROC analysis to evaluate the diagnostic performance of the LFI for liver fibrosis assessment. In HCV-infected patients, the diagnostic accuracy was 73.2 at F4, 72.2 at ≥F3, and 67.9 at ≥F2. In HBV-infected patients, the diagnostic accuracy was 73.4 at F4, 76.6 at ≥F3, and 69.5 at ≥F2 (table 5).

Data Mining Analysis

The LFI is the numerical value calculated from HCV. Therefore, by using the LFI and the serological findings for HCV as well as the 11 feature values of RTE and the serological findings for HBV, the decision tree was calculated. The HCV decision tree, which comprises LFI, AST, ALT, GGT, T-Bil, PLT, HA, and type IV collagen, had a diagnostic accuracy of 94.4% for F1, 54.1% for F2, 38.7% for F3, and 81.3% for F4. The HBV decision tree, which comprises COM, CON, IDM, ALT, PLT, INR, and HA, had a diagnostic accuracy of 97.1% for F1, 50.0% for F2, 43.8% for F3, and 80.6% for F4 (fig. 1; table 6).

Discussion

The LFI, which is a multiple regression equation for assessing liver fibrosis using liver fibrosis estimates from biopsy and RTE image feature values obtained from patients with CHC or cirrhosis, is widely used as the primary diagnostic technique with RTE as it can easily be measured with RTE diagnostic equipment. However, few studies have examined differences in RTE images or the LFI due to differences in etiology, and the usefulness of the LFI for etiologies other than HCV has not been sufficiently discussed. In this study, we found that the LFI was significantly higher in HCV- than in HBV-infected patients with the same stage of fibrosis. This was likely influenced by differences in how fibrosis progresses in these etiologies. Specifically, HCV-infected patients develop micronodular cirrhosis, whereas HBV-infected patients develop macronodular cirrhosis. However, in criteria for evaluating pathological fibrosis in viral liver diseases (e.g., the new Inuyama classification), the stage of fibrosis is based on the area where fibrosis develops rather than the amount of fibrosis present. In essence, the amount of fibrosis per unit of area would be higher in HCV- than in HBV-infected patients with the same stage of fibrosis because the progression of HCV-related fibrosis is micronodular, thereby making the LFI higher as well. When using the LFI, the etiology of the patient must be confirmed before assessing the fibrosis stage.

Although evaluation using AUROC yields a somewhat high diagnostic accuracy for liver fibrosis assessment by the LFI, the stage of fibrosis when using LFI alone in clinical practice is often not exactly clear due to the large amount of overlap in the LFI between stages. Whereas AUROC can be used only to evaluate the diagnostic performance of assessment between two choices, namely ≥F2/F1, ≥F3/≤F2 or F4/≤F3, the decision tree can assess the exact stage of fibrosis (i.e., F1, F2, F3 or F4). Furthermore, the decision tree constructed in this study can be used to determine the specific stage of liver fibrosis based on etiology, serological findings, and RTE findings with very high diagnostic accuracy of each fibrosis stage, suggesting its utility in clinical practice as well. However, the sample size in the F2

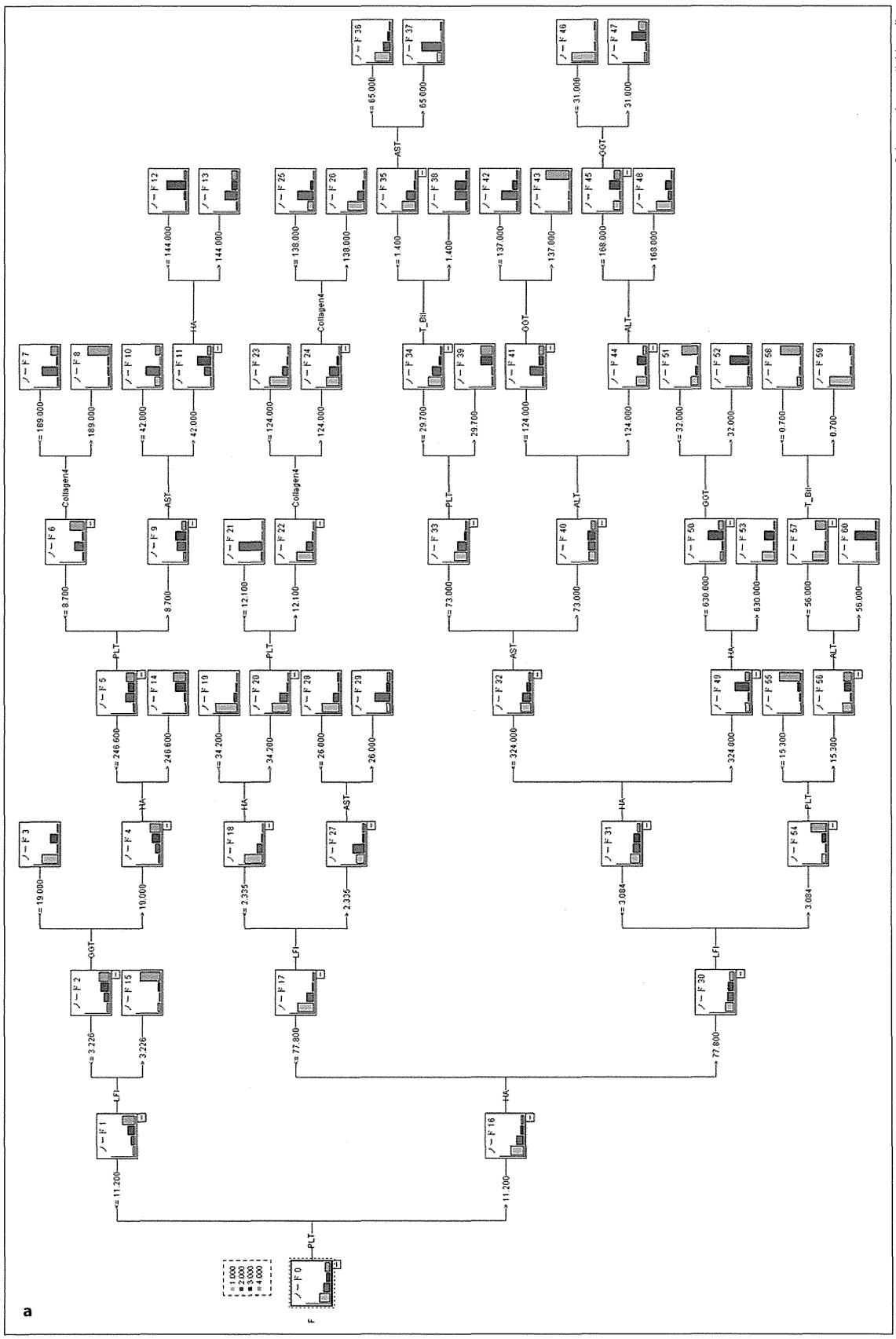

1

(For legend see next page.)

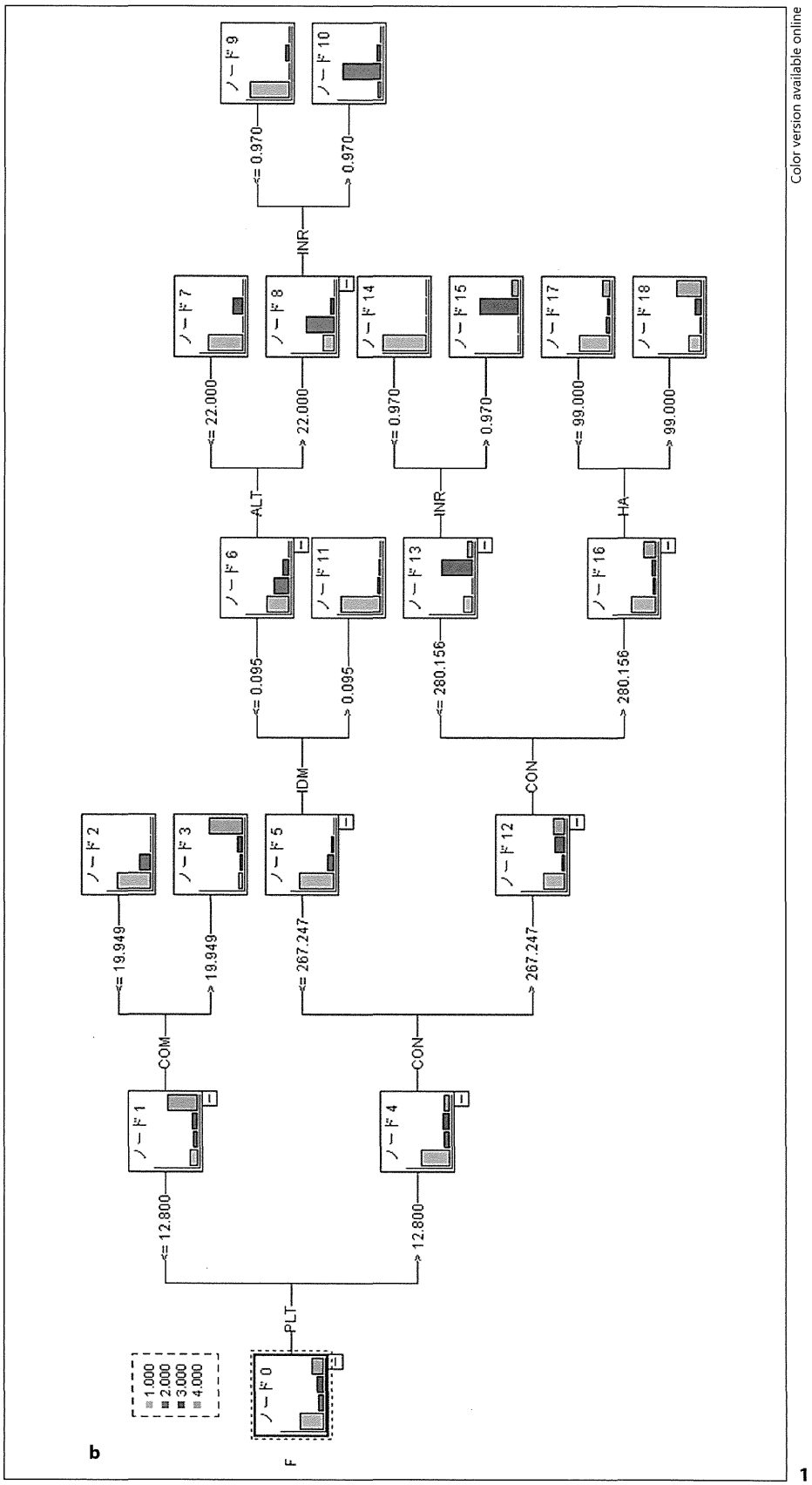

Fig. 1. Data mining for the diagnosis of the fibrosis stage in chronic viral hepatitis: fibrosis diagnosis of CHC (**a**) and CHB (**b**). Each bar graph shows the percentage of cases. The pale blue, red, blue, and green bars represent F1, F2, F3, and F4 fibrosis stage, respectively (colors refer to the online version only). T_Bil = Total bilirubin; Collagen4 = type IV collagen.

Table 6. Diagnostic performance of data mining with both ultrasound elastography and serological findings

	Data mining diagnosis							
	HCV				HBV			
	F1	F2	F3	F4	F1	F2	F3	F4
Pathological diagnosis								
F1	169 (94.4)	8 (4.5)	0	2 (1.1)	67 (97.1)	0	0	2 (2.9)
F2	42 (42.9)	53 (54.1)	1 (1.0)	2 (2.0)	5 (41.7)	6 (50)	0	1 (8.3)
F3	10 (16.1)	10 (16.1)	24 (38.7)	18 (29.0)	6 (37.5)	0	7 (43.8)	3 (18.8)
F4	3 (4.0)	6 (8.0)	5 (6.7)	61 (81.3)	5 (16.1)	0	1 (3.2)	25 (80.6)

Values are presented as n (%).

or F3 stage is too small both in HCV and HBV, which seems to be the reason of low accuracy of the F2 and F3 fibrosis stage.

In this study, we used the gold standard method of assessing liver fibrosis stage with samples obtained by liver biopsy, but, as mentioned previously, sampling error is more likely with an assessment by liver biopsy than with an assessment of hepatectomy specimens. Therefore, to construct a more accurate decision tree, it would be ideal to make the pathological diagnosis based on the hepatectomy specimens. Furthermore, it is also necessary to try to eliminate discrepancies in assessment between readers, for example, by adding computer-aided pathological diagnosis. In light of these issues, further research must be conducted to enable ultrasound elastography to be used as a tool for obtaining a more accurate diagnosis in clinical practice.

Acknowledgements

This study was supported by Health and Labour Sciences Research Grants for the Research on Hepatitis from the Japanese Ministry of Health, Labour and Welfare. The authors thank those who conducted the patient enrollment, namely Kenji Fujimoto (Division of Clinical Research and Department of Internal Medicine, Minami Wakakayama Medical Center, Tanabe, Japan), Shiho Miyase (Department of Gastroenterology and Hepatology, Kumamoto Shinto General Hospital, Kumamoto, Japan), Shunsuke Nojiri (Department of Gastroenterology and Metabolism, Nagoya City University Graduate School of Medical Sciences, Nagoya, Japan), Hideyuki Tamai (Second Department of Internal Medicine, Wakayama Medical University, Wakayama, Japan), Kazuho Imanaka (Department of Hepatobiliary and Pancreatic Oncology, Osaka Medical Center for Cancer and Cardiovascular Diseases, Osaka, Japan), Kazuyoshi Ohkawa (Department of Hepatobiliary and Pancreatic Oncology, Osaka Medical Center for Cancer and Cardiovascular Diseases, Osaka, Japan), Yoichi Hiasa (Department of Gastroenterology and Metabology, Ehime University Graduate School of Medicine, Toon, Japan), Chikara Ogawa (Department of Gastroenterology, Takamatsu Red Cross Hospital, Takamatsu, Japan), Masahiko Koda (Division of Medicine and Clinical Science, Department of Multidisciplinary Internal Medicine, Tottori University School of Medicine, Yonago, Japan), Shuichi Miyase (Department of Gastroenterology, Yatsushiro General Hospital, Yatsushiro, Japan), and Hiroko Iijima (Division of Hepatobiliary and Pancreatic Diseases, Department of Internal Medicine, Hyogo College of Medicine, Nishinomiya, Japan), and Katsuhiko Fukuda (Department of Gastroenterology, PL Hospital, Tondabayashi, Japan).

Disclosure Statement

The authors declare that no financial or other conflicts of interest exist in relation to the content of this article.

References

1 Shiratori Y, Imazeki F, Moriyama M, Yano M, Arakawa Y, Yokosuka O, Kuroki T, Nishiguchi S, Sata M, Yamada G, Fujiyama S, Yoshida H, Omata M: Histologic improvement of fibrosis in patients with hepatitis C who have sustained response to interferon therapy. Ann Intern Med 2000;132:517–524.

2 Yoshida H, Shiratori Y, Moriyama M, Arakawa Y, Ide T, Sata M, Inoue O, Yano M, Tanaka M, Fujiyama S, Nishiguchi S, Kuroki T, Imazeki F, Yokosuka O, Kinoyama S, Yamada G, Omata M: Interferon therapy reduces the risk for hepatocellular carcinoma: national surveillance program of cirrhotic and noncirrhotic patients with chronic hepatitis C in Japan. IHIT study group. Inhibition of Hepatocarcinogenesis by Interferon Therapy. Ann Intern Med 1999;131:174–181.

3 Kim DY, Han KH: Epidemiology and surveillance of hepatocellular carcinoma. Liver Cancer 2012;1:2–14.
4 Kudo M: Early hepatocellular carcinoma: definition and diagnosis. Liver Cancer 2013;2:69–72.
5 Kudo M: Prediction of hepatocellular carcinoma incidence risk by ultrasound elastography. Liver Cancer 2014;3:1–5.
6 Belghiti J, Fuks D: Liver resection and transplantation in hepatocellular carcinoma. Liver Cancer 2012;1:71–82.
7 Chan SC: Liver transplantation for hepatocellular carcinoma. Liver Cancer 2013;2:338–344.
8 Kudo M: Japan's successful model of nationwide hepatocellular carcinoma surveillance highlighting the urgent need for global surveillance. Liver Cancer 2012;1:141–143.
9 Lin SM: Local ablation for hepatocellular carcinoma in Taiwan. Liver Cancer 2013;2:73–83.
10 Bedossa P, Carrat F: Liver biopsy: the best, not the gold standard. J Hepatol 2009;50:1–3.
11 Masuzaki R, Tateishi R, Yoshida H, Yoshida H, Sato S, Kato N, Kanai F, Sugioka Y, Ikeda H, Shiina S, Kawabe T, Omata M: Risk assessment of hepatocellular carcinoma in chronic hepatitis C patients by transient elastography. J Clin Gastroenterol 2008;42:839–843.
12 Masuzaki R, Tateishi R, Yoshida H, Goto E, Sato T, Ohki T, Imamura J, Goto T, Kanai F, Kato N, Ikeda H, Shiina S, Kawabe T, Omata M: Prospective risk assessment for hepatocellular carcinoma development in patients with chronic hepatitis C by transient elastography. Hepatology 2009;49:1954–1961.
13 Jung KS, Kim SU, Ahn SH, Park YN, Kim do Y, Park JY, Chon CY, Choi EH, Han KH: Risk assessment of hepatitis B virus-related hepatocellular carcinoma development using liver stiffness measurement (fibroscan). Hepatology 2011;53:885–894.
14 Fujimoto K, Wada S, Oshita M, Kato M, Tonomura A, Mitake T: Non-invasive evaluation of hepatic fibrosis in patients with chronic hepatitis C using elastography. Medix 2007;(suppl):24–27.
15 Tatsumi C, Kudo M, Ueshima K, Kitai S, Takahashi S, Inoue T, Minami Y, Chung H, Maekawa K, Fujimoto K, Akiko T, Takeshi M: Noninvasive evaluation of hepatic fibrosis using serum fibrotic markers, transient elastography (FibroScan) and real-time tissue elastography. Intervirology 2008;51(suppl 1):27–33.
16 Shiina T, Maki T, Yamakawa M, Mitake T, Kudo M, Fujimoto K: Mechanical model analysis for quantitative evaluation of liver fibrosis based on ultrasound tissue elasticity imaging. Jpn J Appl Phys 2012;51:1–8.
17 Fujimoto K, Kato M, Tonomura A, Yada N, Tatsumi C, Oshita M, Wada S, Ueshima K, Ishida T, Furuta T, Yamasaki M, Tsujimoto M, Motoki M, Mitake T, Shiina T, Kudo M, Hayashi N: Non-invasive evaluation method of the liver fibrosis using real-time tissue elastography – usefulness of judgment liver fibrosis stage by liver fibrosis index (LF index) (in Japanese). Kanzo 2010;59:539–541.
18 Fujimoto K, Kato M, Kudo M, Yada N, Shiina T, Ueshima K, Yamada Y, Ishida T, Azuma M, Yamasaki M, Yamamoto K, Hayashi N, Takehara T: Novel image analysis method using ultrasound elastography for non-invasive evaluation of hepatic fibrosis in patients with chronic hepatitis C. Oncology 2013;84(suppl 1):3–12.
19 Yada N, Kudo M, Morikawa H, Fujimoto K, Kato M, Kawada N: Assessment of liver fibrosis with real-time tissue elastography in chronic viral hepatitis. Oncology 2013;84(suppl 1):13–20.
20 Kudo M, Shiina T, Moriyasu F, Iijima H, Tateishi R, Yada N, Fujimoto K, Morikawa H, Hirooka M, Sumino Y, Kumada T: JSUM ultrasound elastography practice guidelines: liver. J Med Ultrason 2013;40:325–357.
21 Ichida F, Tsuji T, Omata M, Ichida T, Inoue K, Kamimura T, Yamada G, Hino K, Yokosuka O, Suzuki H: New Inuyama classification; new criteria for histological assessment of chronic hepatitis. Int Hepatol Commun 1996;6:112–119.
22 Tatsumi C, Kudo M, Ueshima K, Kitai S, Ishikawa E, Yada N, Hagiwara S, Inoue T, Minami Y, Chung H, Maekawa K, Fujimoto K, Kato M, Tonomura A, Mitake T, Shiina T: Non-invasive evaluation of hepatic fibrosis for type C chronic hepatitis. Intervirology 2010;53:76–81.
23 Shiina T: JSUM ultrasound elastography practice guidelines: basics and terminology. J Med Ultrason 2013;40:309–323.

Hepatology Research

Hepatology Research 2014; 44: 1320–1328 doi: 10.1111/hepr.12307

Original Article

Clinical outcome and prognostic factors of patients with hepatocellular carcinoma and extrahepatic metastasis treated with sorafenib

Tomokazu Kawaoka, Hiroshi Aikata, Hiromi Kan, Hatsue Fujino, Takayuki Fukuhara, Tomoki Kobayashi, Noriaki Naeshiro, Daisuke Miyaki, Akira Hiramatsu, Michio Imamura, Yoshiiku Kawakami, Hideyuki Hyogo and Kazuaki Chayama

Department of Medicine and Molecular Science, Division of Frontier Medical Science, Hiroshima University, Hiroshima, Japan

Aim: The purpose of this study was to assess the clinical outcome and identify prognostic factors following treatment of patients with advanced hepatocellular carcinoma (HCC) and extrahepatic metastasis with sorafenib.

Methods: Sixty-one HCC patients with extrahepatic metastasis who were treated with sorafenib were enrolled in this retrospective cohort study.

Results: The median survival time (MST) of all patients was 11 months. The median time to radiological progression was 4.2 months. The response rates (complete response [CR] + partial response [PR]) by Response Evaluation Criteria in Solid Tumors (RECIST) and modified RECIST were 3.0% and 8.0%, respectively, while the disease control rates (CR + PR + stable disease) were 49% and 49%, respectively. Multivariate analysis identified T factor (intrahepatic tumor stage, T 0–2), response to disease control and des-γ-carboxy prothrombin (<2600 mAU/mL) as significant and independent determinants of survival. Intrahepatic tumor stage before treatment allows stratification of prognosis of patients treated with sorafenib. Four T0 patients remained alive. The MST of patients with T1 (n = 6), T2 (n = 10), T3 (n = 23) and T4 (n = 18) of intrahepatic tumor stage was 20, 23, 7 and 5 months, respectively. Among the progressive disease group, patients with T0–2 intrahepatic tumor stage had better prognosis than patients with T3–4.

Conclusion: In HCC patients with extrahepatic metastasis who are treated with sorafenib, intrahepatic tumor stage was a significant and independent prognostic factor.

Key words: extrahepatic metastasis, hepatocellular carcinoma, intrahepatic tumor stage, sorafenib

INTRODUCTION

HEPATOCELLULAR CARCINOMA (HCC) is one of the most common malignant tumors worldwide.[1–4] Infection with hepatitis B or C virus is a risk factor for hepatocarcinogenesis. Sorafenib is the current standard drug for systemic treatment of patients with advanced HCC who are not candidates for curative treatments, such as surgical resection or locoregional therapies.[5,6] This multikinase inhibitor, with activities against Raf kinase and vascular endothelial cell growth factor receptor, has been approved for the treatment of unresectable HCC by the regulatory agencies of the European Union, the USA and other countries.[7] The approval was based on the positive results of a placebo-controlled randomized phase III study of patients with advanced HCC.[5] Subsequently, a phase III study conducted in the Asia–Pacific region, where hepatitis B virus infection is the predominant etiologic factor for chronic liver disease, also demonstrated the survival benefits of sorafenib.[8] For patients with advanced stage HCC and extrahepatic metastasis, sorafenib is currently the only standard treatment in many Western and Eastern countries. However, only a few studies have reported the clinical outcome of sorafenib treatment in HCC patients with extrahepatic metastasis.

A substudy of the Sorafenib Hepatocellular Carcinoma Assessment Randomized Protocol (SHARP)

Correspondence: Dr Hiroshi Aikata, Department of Medicine and Molecular Science, Division of Frontier Medical Science, Programs for Biomedical Research, Graduate School of Biomedical Sciences, Hiroshima University, 1-2-3 Kasumi, Minami-ku, Hiroshima 734-8551, Japan. Email: aikata@hiroshima-u.ac.jp
Received 17 November 2013; revision 8 January 2014; accepted 26 January 2014.

reported that the overall survival (OS) and time to progression (TTP) of group C with Barcelona Clinic Liver Cancer (BCLC) staging criteria were 9.7 and 4.9 months, respectively.[8] To our knowledge, however, there is no study that have examined the outcome of sorafenib treatment in patients with metastatic HCC only. A phase III study conducted in the Asia–Pacific region reported that OS and TTP of patients with lung metastasis were 5.6 and 2.4 months, respectively, while those of patients with lymph metastasis were 5.6 and 2.8 months, respectively.[9]

To date, the prognostic factors remain unclear in patients with extrahepatic metastasis. In general, the stage of intrahepatic tumors could vary extensively in HCC patients with extrahepatic metastasis, with some patients having only extrahepatic tumors with tumor-free liver tissue, while others have advanced intrahepatic tumors. These differences could affect the clinical outcome of sorafenib treatment. In fact, several studies on the clinical outcome of patients with advanced HCC and extrahepatic metastasis who received non-sorafenib therapy demonstrated that intrahepatic tumor progression was a significant prognostic factor.[4,10–12] Whether the same applies to sorafenib treatment remains to be determined. Specifically, the difference in the response to sorafenib between patients with intrahepatic tumors and those with extrahepatic tumors remains obscure.

Clinical evidence suggests that sorafenib therapy is suitable for HCC patients with extrahepatic metastasis, as demonstrated by the positive results of the placebo-controlled randomized phase III study, SHARP study and Asia–Pacific study of patients with advanced HCC.[5,8] However, these studies reported poor prognosis of HCC patients with extrahepatic metastasis compared to those without extrahepatic metastasis. For the development of new therapies that can improve the prognosis of such patients, there is a need to study the clinical outcome and prognosis of patients with extrahepatic metastasis treated with sorafenib.

The present retrospective study assessed the clinical outcome and prognostic factors in patients with advanced HCC and extrahepatic metastasis treated with sorafenib.

METHODS

Patients

THE SUBJECTS OF this retrospective cohort study were all 61 HCC patients with extrahepatic metastasis who had been treated with sorafenib at Hiroshima University between June 2009 and September 2012. These subjects were considered unfit for surgery, liver transplantation, repeat locoregional therapy, repeat transcatheter arterial chemoembolization (TACE) or repeat hepatic arterial infusion chemotherapy (HAIC). The inclusion criteria for treatment with sorafenib were Eastern Cooperative Oncology Group performance status (ECOG PS) score of 2 or less, Child–Pugh liver function class A and adequate hematological function (platelet count, $\geq 5 \times 10^4/\mu L$; hemoglobin, ≥8.5 g/dL), adequate hepatic function (albumin, ≥2.8 g/dL; total bilirubin, ≤3 mg/dL; and alanine aminotransferase and aspartate aminotransferase, ≤5 times the upper limit of the normal range), and adequate renal function (serum creatinine, ≤1.5 times the upper limit of the normal range) according to the SHARP study.[5]

The clinical characteristics of the study group are summarized in Table 1. With regard to treatment received before sorafenib, 18 patients were naïve to HCC treatment, eight were non-responders to TACE, 12 non-responders to HAIC and 23 non-responders to systemic chemotherapy. All patients were Child–Pugh A. Intrahepatic tumor stage was based on the Liver Cancer Study Group of Japan/Tumor–Node–Metastasis staging system of the Liver Cancer Study Group of Japan.[13] Stage I was defined by the presence of: (i) a solitary tumor; (ii) measuring less than 2 cm in diameter; and (iii) without any vessel invasion ($n = 0$; 0%). Stage II fulfilled two of the above three features ($n = 0$, 0%), stage III fulfilled one of the above three conditions ($n = 0$, 0%), stage IVa fulfilled none of the above three, with no distant metastasis or intrahepatic condition with lymph node metastasis ($n = 8$, 13%), and those with stage IVb fulfilled none of the above features with distant metastasis ($n = 53$, 87%).

As for the T factor, patients with T0 had no hepatic tumor ($n = 4$, 6%), tumors in patients with T1 fulfilled three features (with a solitary tumor measuring <2 cm in diameter with no vessel invasion) ($n = 6$, 9%), T2 fulfilled two of the above three features ($n = 10$, 16%), T3 fulfilled one of the above three conditions ($n = 23$, 37%) and stage T4 fulfilled none of the above three ($n = 18$, 32%).

The study was conducted in accordance with the Declaration of Helsinki and the study protocol was approved by the ethics committee of our hospital. Written informed consent was obtained from each participating patient.

Treatment regimens

All patients commenced treatment with sorafenib between June 2009 and September 2012, at a dose of

Table 1 Baseline characteristics of 61 HCC patients with extrahepatic metastasis treated with sorafenib

Age (years)	64 (20–79)
Sex (males/females)	56/5
Performance status (0/1/2/3)	50/9/1/1
Etiology (HBV/HCV/non-HBV, non-HCV)	30/18/13
Total bilirubin (mg/dL)*	0.8 (0.4–1.8)
Albumin (g/dL)*	3.9 (2.8–4.9)
Platelet count ($\times 10^4/\mu L$)*	13.5 (6.3–30.1)
Child–Pugh (A/B)	61/0
HCC stage (IVa/IVb)	8/53
Size of hepatic tumor (mm) (range)	30 (0–194)
Intrahepatic tumor stage T (0/1/2/3/4)	4/6/10/23/18
No. of hepatic tumors (1–2/≥3)	23/38
Vp (0–2/3–4)	47/14
Tumor size relative to the liver (≤50%/>50%)	44/17
AFP (ng/mL)*	290 (<5–2 650 000)
DCP (mAU/mL)*	2684 (13–4 376 200)
No. of organs with extrahepatic metastasis (1/2/3/4)	39/18/3/1
No. of extrahepatic metastasis lesion	4 (1–102)
Organ with metastases (lung/LN/bone/adrenal/peritoneum/pleura/fascia/kidney)	39/20/15/5/3/1/1/1
Treatment before sorafenib (systemic chemotherapy/HAIC/TACE/none)	23/12/8/18

Data are median (range).
AFP, α-fetoprotein; DCP, des-γ-carboxy prothrombin; HAIC, hepatic arterial infusion chemotherapy; HCC, hepatocellular carcinoma; HBV, hepatitis B virus; HCV, hepatitis C virus; LN, lymph nodes; TACE, transcatheter arterial chemoembolization; Vp 0, no tumor thrombus; Vp, one tumor thrombus in the second branch of the portal vein; Vp 3, tumor thrombus in the first branch of the portal vein; Vp 4, tumor thrombus in the trunk of the portal vein.

400 mg twice daily (standard dose). Treatment interruptions and dose reductions (400 mg once daily) were permitted for adverse drug reactions. Patients continued therapy until death or met one of the following criteria for cessation of therapy: (i) adverse events that required termination of treatment; (ii) deterioration of ECOG PS to 4; (iii) worsening liver function; or (iv) withdrawal of consent. The criteria of liver function for the discontinuation of treatment was total bilirubin of more than 3 mg/dL at 4 weeks after cessation of treatment. Even if patients developed progressive disease with sorafenib, sorafenib was continued to a maximum extent. After progressive disease with sorafenib, second-line treatment or local treatment was not administrated to patients.

Assessment of response to therapy

Minimal treatment duration was considered 8 weeks in the present study. In patients who continued sorafenib therapy for more than 8 weeks, the response to treatment was evaluated by the Response Evaluation Criteria in Solid Tumors (RECIST) and modified RECIST (mRECIST) at 8 weeks. Subsequently, each patient underwent dynamic computed tomography or magnetic resonance imaging every 2–3 months. OS was assessed from the date of commencement of sorafenib therapy until the date of death from any cause. The time to radiologic tumor progression was defined as the time from the date of commencement of sorafenib therapy to disease progression, as assessed by RECIST and mRECIST. We defined the minimal time interval for determination of stable disease as 8 weeks.

The concentrations of serum tumor markers α-fetoprotein and des-γ-carboxy prothrombin (DCP) were measured once a month after the start of sorafenib treatment.

Follow-up protocol

Safety assessments included documentation of adverse drug reactions, clinical laboratory tests, physical examination and measurement of vital signs. Adverse drug reactions were defined according to the Common Terminology Criteria for Adverse Events version 4.0 (CTCAE v4.0; http://ctep.cancer.gov).

Statistical analysis

Continuous variables were presented as mean ± standard deviation, while categorical variables were pre-

sented as absolute and relative frequencies. The time to radiologic tumor progression and OS were calculated by Kaplan–Meier survival curves with log-rank survival comparisons and 95% confidence intervals (95% CI). A Cox proportional hazards model was used to investigate the prognostic factors for OS. $P < 0.05$ denoted the presence of statistically significant difference. We set cut-off values of continuous variables on median. The median of number of organs with metastases was one. Therefore, we made the separation of 1 versus 2–4. According to the macroscopic vascular invasion effect of survival in the SHARP study, we made the separation of Vp 0–2 versus 3–4, because the major branch of the portal vein is Vp 3–4. All statistical analyses were carried out with the Predictive Analytics Software version 21.0 (SPSS, Chicago, IL, USA).

RESULTS

Sorafenib treatment

THE MEDIAN DURATION of sorafenib therapy was 5.3 months (range, 0.1–41.3), with a median follow-up period of 8.1 months (range, 0.3–41.3). Treatment was terminated within 8 weeks in four patients due to side-effects (6%).

Safety and tolerability

The drug-related grade 3/4 adverse effects encountered in this study were hand–foot skin reactions in one (1.0%) patient, diarrhea in three (4%), general fatigue in one (1.0%) and perforation of the colon in one (1%). As stated above, three of the four adverse effects were the reason for cessation of treatment within 8 weeks in one patient (perforation of the colon).

Efficacy and response to treatment

The response to sorafenib therapy was evaluated by RECIST and mRECIST at 8 weeks from the date of administration of sorafenib. Four patients could not be evaluated because treatment was terminated within 8 weeks in four patients due to side-effects. Based on RECIST, the response to therapy was assessed as partial response (PR) in two patients, and stable disease (SD) in 28. The response rate, defined as percentage of patients who showed complete response (CR) or PR, was 3%, and the disease control rate was 49%. Based on mRECIST, CR was noted in one patient, PR in four and SD in 25, with a response rate (CR + PR) of 8% and disease control rate of 49%. One patient evaluated as PR by RECIST was evaluated as CR by mRECIST, while two patients evaluated as SD by RECIST were evaluated as PR by mRECIST. The median time to radiologic tumor progression was 4.2 months by RECIST as well as mRECIST (Fig. 1a).

Among all 27 PD patients, 10 patients were considered to have shown extrahepatic tumor progression only without intrahepatic tumor progression, while the remaining 17 patients showed intrahepatic tumor progression.

Survival

The median survival time (MST) of the entire group was 11 months (Fig. 1b). The MST of patients who showed PR, SD, PD and not evaluated (NE) was 20, 28, 5 and 3 months, respectively, by RECIST. On the other hand, the MST of CR, PR, SD, PD and NE patients was 20, 13, 15, 5 and 3 months by mRECIST, respectively. Assessment by mRECIST ($P < 0.0001$) provided a similar stratification of patients according to OS, compared with assessment by RECIST ($P < 0.0001$).

The MST of HCC patients with lung, lymph and bone metastasis was 13, 9.4 and 9.4 months, respectively.

Survival according intrahepatic tumor stage

The survival rate was also stratified by intrahepatic tumor stage ($P = 0.003$) (Fig. 2). All four T0 patients were alive during the follow-up period. The MST of patients with T1 ($n = 6$), T2 ($n = 10$), T3 ($n = 23$) and T4 ($n = 18$) for intrahepatic tumor staging was 20, 23, 7 and 5 months, respectively. The survival rate worsened with the progression of intrahepatic tumors. Assessment of OS by Vp showed that the rate of Vp 0–2 was significantly better than that of Vp 3–4 ($P = 0.004$). The MST of 47 patients with Vp 0–2 was 12 months while that of 14 patients with Vp 3–4 was 4 months (Fig. 3). Among the disease control group (CR, PR and SD), patients with T0–2 of intrahepatic stage (MST, 21 months) tended to show a better survival than those with T3–4 (MST, 13 months), although the difference was not significant ($P = 0.088$) (Fig. 4a). On the other hand, among the disease PD group, patients with T0–2 of intrahepatic tumor stage (MST, 14 months) showed a significantly better survival than those with T3–4 (MST, 7 months) ($P = 0.035$) (Fig. 4b).

Determinants of OS

Finally, in 61 patients we investigated the relationship between survival of the entire group after initiation of sorafenib therapy and various clinicopathological variables by univariate analysis. Etiology ($P = 0.044$), DCP ($P = 0.004$), T0–2 of intrahepatic tumor stage ($P =$

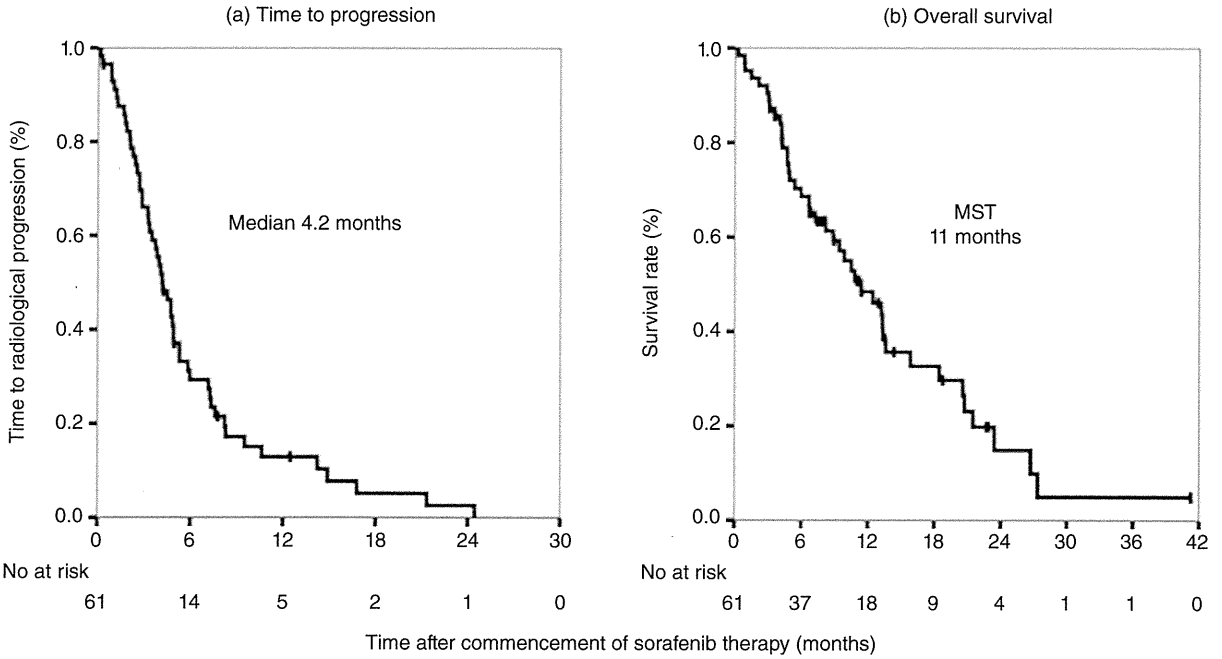

Figure 1 Time to radiological progression and overall survival rate in patients treated with sorafenib. (a) The median time to radiological progression was 4.2 months. (b) The median survival time for all patients was 11 months.

0.006) and response to disease control ($P = 0.0001$) correlated significantly with OS. The above parameters were then entered into multiple Cox proportional hazard model analysis. Multivariate analysis identified response to disease control ($P = 0.001$), T0–2 of intrahepatic tumor stage (0–2) ($P = 0.0001$) and DCP (<2600 mAU/mL) ($P = 0.046$) as significant and independent determinants of OS (Table 2).

We also investigated the relationship between survival of 27 PD patients after initiation of sorafenib therapy and various clinicopathological variables by univariate analysis. T0–2 of intrahepatic tumor stage ($P = 0.035$) and lymph node metastasis ($P = 0.048$) correlated significantly with OS. The above parameters were then entered into multiple Cox proportional hazard model analysis. Multivariate analysis identified T0–2 of intrahepatic tumor stage (hazard ratio [HR], 3.3; 95% CI, 1.1–10; $P = 0.047$) as significant and independent determinant of survival (Table 3).

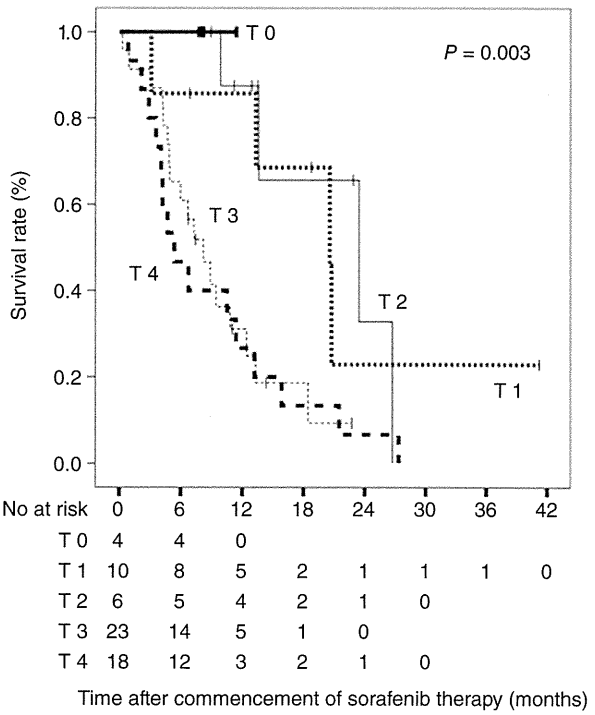

Figure 2 Survival rate stratified by hepatic tumor.

DISCUSSION

IN THE PRESENT study, the prognosis of HCC patients with extrahepatic metastasis was stratified by intrahepatic tumor progression. Worsening of intra-

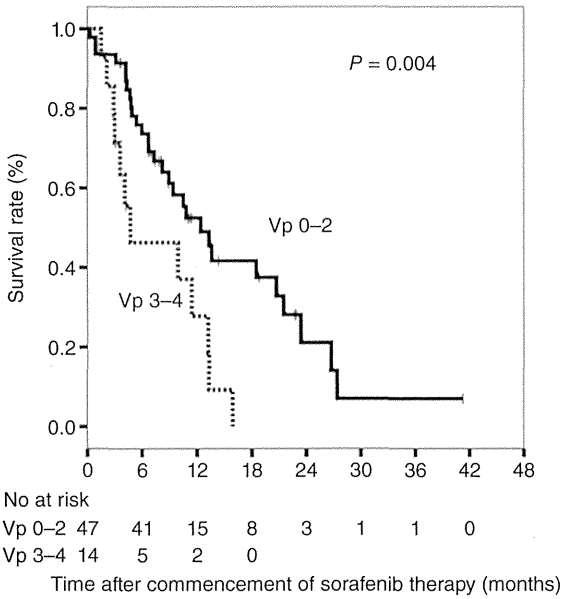

Figure 3 Overall survival rate by Vp 0–2 or Vp 3–4.

hepatic tumor stage was associated with poor prognosis of patients with extrahepatic metastasis. In addition, some patients showed different response of intrahepatic tumors compared with extrahepatic tumors. For example, good prognosis was noted in intrahepatic tumor with poor response of extrahepatic tumor.

In a phase III study conducted in the Asia–Pacific region, the OS and TTP of patients with lung metastasis were 5.6 and 2.4 months, respectively. On the other hand, the OS and TTP of patients with lymph metastasis were 5.6 and 2.8 months, respectively.[8] Our results showed that the MST of 13 HCC patients with lung, lymph and bone metastasis was 13, 9.4 and 9.4 months, respectively. These findings point to better results compared with the phase III study conducted in the Asia–Pacific region. The reason for the better outcome could be due to differences in the population sample with intrahepatic tumor progression. In the PD group, intrahepatic tumor progression was identified as a significant prognostic factor in HCC patients with extrahepatic metastasis.

Previous studies examined the clinical outcome of HCC patients with extrahepatic metastasis treated by modalities other than sorafenib. Uka *et al.*[10] examined patients with intrahepatic tumor stage T0–2 and concluded that those free of portal venous invasion but with extrahepatic metastasis showed improved survival. On the other hand, Uchino *et al.*[11] reported that the control of intrahepatic lesions and performance status were significant prognostic factors in patients with advanced HCC and extrahepatic metastasis. Our results also identified intrahepatic tumor stage as a significant prognostic

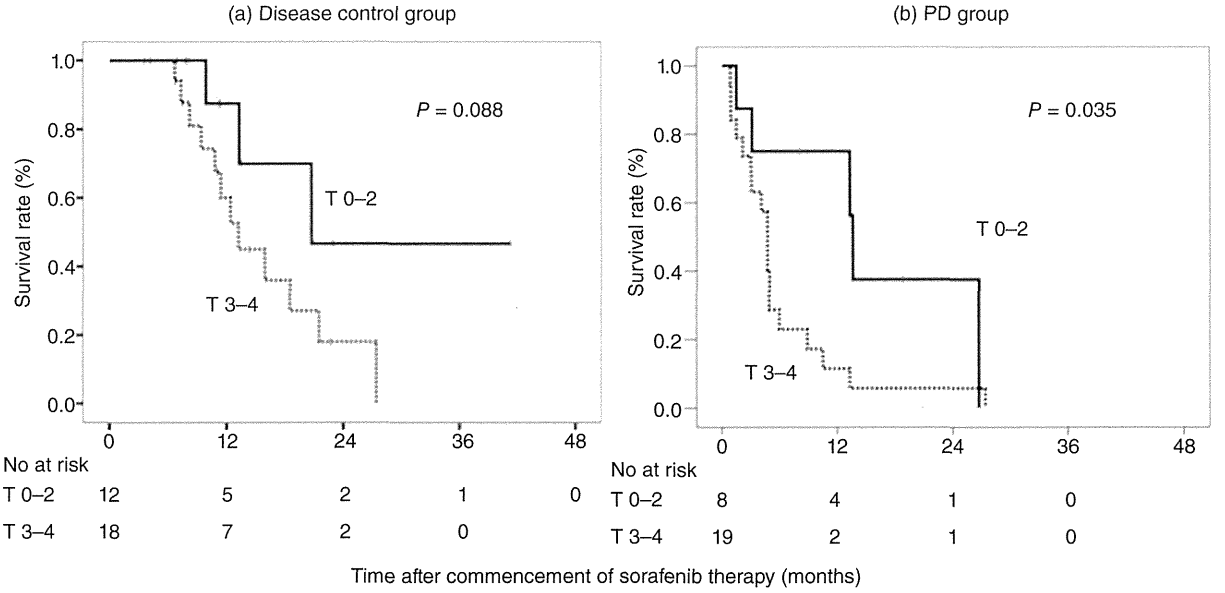

Figure 4 Overall survival according to intrahepatic tumor stage in the (a) disease control group and (b) progressive disease group.

Table 2 Results of univariate and multivariate analyses for prognostic factors in 61 HCC patients with extrahepatic metastases treated with sorafenib

Variable	95% CI	*P*	HR	95% CI	*P*
Age (<65 vs ≥65 years)	0.3–1.1	0.1			
Sex (males vs females)	0.2–2.6	0.8			
Performance status (0–1 vs 2–3)	0.7–3.3	0.2			
Etiology (others vs HBV)	1.0–3.5	0.044			
Platelet count ($\times 10^4/\mu L$) (<25 vs ≥25)	0.2–5.3	0.2			
Intrahepatic tumor stage T(0–2 vs 3–4)	2–10	0.006	8.3	2.1–10.1	0.0001
AFP (ng/mL)* (<300 vs ≥300)	0.9–3.1	0.09			
DCP (mAU/mL)* (<2600 vs ≥2600)	1.3–4.9	0.004	1.9	1.01–3.8	0.046
Treatment before sorafenib (no vs yes)	0.2–1.0	0.07			
No. of organs with metastases (1 vs 2–4)	0.6–2.4	0.4			
No. of extrahepatic metastasis lesion (1–4 vs 5–102)	0.5–1.8	0.9			
Lung metastasis (no vs yes)	0.2–1.0	0.053			
Bone metastasis (no vs yes)	0.6–2.7	0.3			
Lymph node metastasis (no vs yes)	0.8–2.9	0.1			
Response to disease control	2–10	0.0001	6.25	2.5–11.1	0.0001

Patients with T0 had no hepatic tumor, tumors of patients with T1 had three features (with a solitary tumor measuring <2 cm in diameter with no vessel invasion), those with T2 fulfilled two of the above three features, while those with T3 fulfilled one of the above three conditions and stage T4 fulfilled none of the above three.
AFP, α-fetoprotein; CI, confidence interval; DCP, des-γ-carboxy prothrombin; HBV, hepatitis B virus; HR, hazard ratio.

factor in HCC patients with extrahepatic metastasis treated with sorafenib.

We demonstrated that DCP was one of the independent factors related with survival in Table 2. DCP is a well-known tumor marker of HCC,[14] the expression of which is significantly correlated with poor prognosis,[15–17] which is the same in sorafenib treatment for HCC patients with extrahepatic metastasis.

According to the current guidelines applied in Western (BCLC) and Eastern (i.e. the Liver Cancer Study

Table 3 Results of univariate and multivariate analyses for prognostic factors in 27 PD patients

Variable	95% CI	*P*	HR	95% CI	*P*
Age (<65 vs ≥65)	0.6–3.5	0.3			
Sex (males vs females)	0.1–2.9	0.6			
Performance status (0–1 vs 2–3)	0.6–6.3	0.2			
Etiology (others vs HBV)	0.4–2.7	0.8			
Platelet count ($\times 10^4/\mu L$) (<25 vs ≥25)	0.5–3.1	0.5			
Intrahepatic tumor stage T (0–2 vs 3–4)	1.1–8.3	0.035	3.3	1.1–10	0.047
AFP (ng/mL)* (<300 vs ≥300)	0.5–3.2	0.4			
DCP (mAU/mL)* (<2600 vs ≥2600)	0.6–4.2	0.3			
Treatment before sorafenib (no vs yes)	0.2–1.1	0.1			
No. of organs with metastases (1 vs 2–4)	0.9–5.2	0.08			
No. of extrahepatic metastasis lesions (1–4 vs 5–102)	0.6–3.2	0.4			
Lung metastasis (no vs yes)	0.4–2.7	0.7			
Bone metastasis (no vs yes)	0.4–3.0	0.8			
Lymph node metastasis (no vs yes)	0.9–5.6	0.048			

Patients with T0 had no hepatic tumor, tumors of patients with T1 had three features (with a solitary tumor measuring <2 cm in diameter with no vessel invasion), those with T2 fulfilled two of the above three features, while those with T3 fulfilled one of the above three conditions and stage T4 fulfilled none of the above three.
AFP, α-fetoprotein; CI, confidence interval; DCP, des-γ-carboxy prothrombin; HBV, hepatitis B virus; HR, hazard ratio.

Group of Japan) countries,[13,18] sorafenib is the only treatment available for patients with HCC and metastasis. On the other hand, the results of the present study and those of previous reports indicate that the control and/or down-staging of intrahepatic tumors by locoregional therapy (e.g. resection or ablation) seems to improve prognosis of patients with HCC metastasis. However, when extrahepatic metastatic lesions pose a clear threat to health (e.g. respiratory failure in the presence of multiple lung metastases), there is a need to treat such extrahepatic lesions by local therapy and/or systemic sorafenib therapy, without the need to continue locoregional therapy of intrahepatic tumors. The new finding of the present study was that in HCC patients with extrahepatic metastasis treated with sorafenib, intrahepatic tumor stage was a significant and independent prognostic factor.

For the further improvement of survival in patients with extrahepatic metastasis, in addition to sorafenib therapy, combination therapy (e.g. locoregional therapy, TACE, HAIC) with sorafenib may be necessary for intrahepatic tumor according to T factor.

This study indicates that a further clinical study of treatment of intrahepatic tumors in HCC patients with extrahepatic metastasis may be necessary.

Our results showed that worsening of intrahepatic tumors was associated with poor prognosis of patients with extrahepatic metastasis. The OS of patients with Vp 3–4 was especially poor (MST, 4 months), thus limiting the use of sorafenib therapy for patients with Vp 3–4. In subanalysis of the SHARP study and Asia–Pacific study, macrovascular invasion was identified as a poor prognostic factor even in patients with extrahepatic metastasis.[5,8] On the other hand, HAIC for patients with macrovascular invasion (e.g. Vp 3–4) was reported previously to be associated with a response rate of 30–40%, as well as improvement of prognosis of patients with disease control.[19–24] The response to HAIC before sorafenib therapy may improve the prognosis of patients with extrahepatic metastasis and Vp 3–4. These issues are currently being examined in two ongoing clinical trials; the HICS 55 (UMIN000009094) and SCOOP-α (UMIN000006147).

Previous studies reported poor response and OS of patients with Vp 3–4 and extrahepatic metastasis compared to that of patients without extrahepatic metastasis.[25] Patients who show poor response to HAIC need to be switched to sorafenib therapy. In this regard, the Randomized Controlled Trial Comparing Efficacy of Sorafenib versus Sorafenib in Combination with Low-dose Cisplatin/Fluorouracil Hepatic Arterial Infusion Chemotherapy in Patients with Advanced Hepatocellular Carcinoma (SILIUS Phase III) (UMIN000004315) is currently underway. Improvement of such therapy may render it suitable for patients with extrahepatic metastasis with Vp 3–4.

In conclusion, the results of the present study demonstrated that intrahepatic tumor stage was a significant and independent prognostic factor in HCC patients with extrahepatic metastasis treated with sorafenib. Although the sample number is relatively small, the results may help establish a new treatment strategy in patients with HCC-related extrahepatic metastasis.

REFERENCES

1 Taylor-Robinson SD, Foster GR, Arora S, Hargreaves S, Thomas HC. Increase in primary liver cancer in the UK, 1979-94. *Lancet* 1997; **350:** 1142–3.
2 El-Serag HB, Mason AC. Rising incidence of hepatocellular carcinoma in the United States. *N Engl J Med* 1999; **340:** 745–50.
3 Okita K. Management of hepatocellular carcinoma in Japan. *J Gastroenterol* 2006; **41:** 100–6.
4 Ishii H, Furuse J, Kinoshita T *et al.* Extrahepatic spread from hepatocellular carcinoma: who are candidates for aggressive anti-cancer treatment? *Jpn J Clin Oncol* 2004; **34:** 733–9.
5 Llovet JM, Ricci S, Mazzaferro V *et al.* Sorafenib in advanced hepatocellular carcinoma. *N Engl J Med* 2008; **359:** 378–90.
6 Kawaoka T, Aikata H, Murakami E *et al.* Evaluation of the mRECIST and alpha-fetoprotein ratio for stratification of the prognosis of advanced-hepatocellular-carcinoma patients treated with sorafenib. *Oncology* 2012; **83:** 192–200.
7 Wilhelm SM, Carter C, Tang L *et al.* BAY 43-9006 exhibits broad spectrum oral antitumor activity and targets the RAF/MEK/ERK pathway and receptor tyrosine kinases involved in tumor progression and angiogenesis. *Cancer Res* 2004; **64:** 7099–109.
8 Cheng AL, Kang YK, Chen Z *et al.* Efficacy and safety of sorafenib in patients in the Asia-Pacific region with advanced hepatocellular carcinoma: a phase III randomised, double-blind, placebo-controlled trial. *Lancet Oncol* 2009; **10:** 25–34.
9 Cheng AL, Guan Z, Chen Z *et al.* Efficacy and safety of sorafenib in patients with advanced hepatocellular carcinoma according to baseline status: subset analyses of the phase III Sorafenib Asia-Pacific trial. *Eur J Cancer* 2012; **48:** 1452–65.
10 Uka K, Aikata H, Takaki S *et al.* Clinical features and prognosis of patients with extrahepatic metastases from hepatocellular carcinoma. *World J Gastroenterol* 2007; **13:** 414–20.

11 Uchino K, Tateishi R, Shiina S *et al.* Hepatocellular carcinoma with extrahepatic metastasis: clinical features and prognostic factors. *Cancer* 2011; **1** (117): 4475–83.
12 Natsuizaka M, Omura T, Akaike T *et al.* Clinical features of hepatocellular carcinoma with extrahepatic metastases. *J Gastroenterol Hepatol* 2005; **20**: 1781–7.
13 The general rules for the clinical and pathological study of primary liver cancer. Liver Cancer Study Group of Japan. *Jpn J Surg* 1989; **19**: 98–129.
14 Gomaa AI, Khan SA, Leen EL, Waked I, Taylor-Robinson SD. Diagnosis of hepatocellular carcinoma. *World J Gastroenterol* 2009; **21**: 1301–14.
15 Kobayashi M, Ikeda K, Kawamura Y *et al.* High serum des-gamma-carboxy prothrombin level predicts poor prognosis after radiofrequency ablation of hepatocellular carcinoma. *Cancer* 2009; **115**: 571–80.
16 Miyaaki H, Nakashima O, Kurogi M, Eguchi K, Kojiro M. Lens culinaris agglutinin-reactive alpha-fetoprotein and protein induced by vitamin K absence II are potential indicators of a poor prognosis: a histopathological study of surgically resected hepatocellular carcinoma. *J Gastroenterol* 2007; **42**: 962–8.
17 Nagaoka S, Yatsuhashi H, Hamada H *et al.* The des-gamma-carboxy prothrombin index is a new prognostic indicator for hepatocellular carcinoma. *Cancer* 2003; **15**: 2671–7.
18 Llovet JM, Bru C, Bruix J. Prognosis of hepatocellular carcinoma: the BCLC staging classification. *Semin Liver Dis* 1999; **19**: 329–38.
19 Uka K, Aikata H, Takaki S *et al.* Pretreatment predictor of response, time to progression, and survival to intraarterial 5-fluorouracil/interferon combination therapy in patients with advanced hepatocellular carcinoma. *J Gastroenterol* 2007; **42**: 845–53.
20 Obi S, Yoshida H, Toune R *et al.* Combination therapy of intraarterial 5-fluorouracil and systemic interferon-alpha for advanced hepatocellular carcinoma with portal venous invasion. *Cancer* 2006; **106**: 1990–7.
21 Miyaki D, Aikata H, Honda Y *et al.* Hepatic arterial infusion chemotherapy for advanced hepatocellular carcinoma according to Child-Pugh classification. *J Gastroenterol Hepatol* 2012; **27**: 1850–7.
22 Uka K, Aikata H, Takaki S *et al.* Similar effects of recombinant interferon-alpha-2b and natural interferon-alpha when combined with intra-arterial 5-fluorouracil for the treatment of advanced hepatocellular carcinoma. *Liver Int* 2007; **27**: 1209–16.
23 Sakon M, Nagano H, Dono K *et al.* Combined intraarterial 5-fluorouracil and subcutaneous interferon-alpha therapy for advanced hepatocellular carcinoma with tumor thrombi in the major portal branches. *Cancer* 2002; **94**: 435–42.
24 Ota H, Nagano H, Sakon M *et al.* Treatment of hepatocellular carcinoma with major portal vein thrombosis by combined therapy with subcutaneous interferon-alpha and intra-arterial 5-fluorouracil; role of type 1 interferon receptor expression. *Br J Cancer* 2005; **93**: 557–64.
25 Katamura Y, Aikata H, Kimura Y *et al.* Intra-arterial 5-fluorouracil/interferon combination therapy for hepatocellular carcinoma with portal vein tumor thrombosis and extrahepatic metastases. *J Gastroenterol Hepatol* 2010; **25**: 1117–22.

IJC
International Journal of Cancer

Fatty liver creates a pro-metastatic microenvironment for hepatocellular carcinoma through activation of hepatic stellate cells

Yoshihiro Mikuriya, Hirotaka Tashiro, Shintaro Kuroda, Junko Nambu, Tsuyoshi Kobayashi, Hironobu Amano, Yuka Tanaka and Hideki Ohdan

Department of Gastroenterological and Transplant Surgery, Applied Life Sciences, Institute of Biomedical & Health Sciences, Hiroshima University, Japan

Fatty liver (FL) is associated with development of hepatocellular carcinoma (HCC). However, whether FL itself promotes the progression of HCC is unclear. We recently found that hepatic stellate cells (HSCs) were prominently activated in the steatotic liver. Here, we investigated whether steatotic livers promote HCC progression and whether HSCs of steatotic liver are associated with HCC progression. We implanted rat HCC cells into diet-induced steatotic livers in rats *via* portal vein injection. Thereafter, HSCs and HCC cells were co-implanted subcutaneously into nude rats. Migration and proliferation of HCC cells were measured, and activation of ERK and Akt in these cells was determined by western blotting. Chemokines secreted from HSCs and HCC cells were also evaluated by ELISA. Steatotic livers significantly promoted HCC metastasis compared with non-steatotic livers. Additionally, co-implantation of HCC cells with HSCs from steatotic livers produced significantly larger tumors in recipient rats as compared to those induced by HCC cells co-implanted with HSCs from normal livers (NLs). HSCs isolated from steatotic livers, compared with HSCs isolated from NLs, secreted greater amounts of interleukin-1α, vascular endothelial growth factor, and transforming growth factor-β. These cytokines may enhance the proliferation and migration of HCC cells by increasing the phosphorylation of ERK and Akt in HCC cells. Moreover, we noted that the Rho-kinase inhibitor deactivated activated HSCs and attenuated HCC progression. In conclusion, the rat steatotic liver microenvironment favors HCC metastasis, and this effect appears to be promoted by activated HSCs in the steatotic liver.

Non-alcoholic fatty liver disease (NAFLD) is one of the most common hepatic disorders in developed countries. The epidemic of obesity in developed countries has increased along with its attendant complications, including metabolic syndrome and NAFLD. Recently, there is increasing evidence that NAFLD, including the more aggressive non-alcoholic steatohepatitis (NASH), is associated with hepatocellular carcinoma (HCC).[1–3] Diabetes and obesity are established independent

Key words: HCC, hepatic stellate cell, fatty liver, Rho-kinase

Abbreviations: CDD: choline-deficient diet; CM: conditioned media; DMEM: Dulbecco's modified Eagle's medium; ELISA: enzyme-linked immunosorbent assay; FL: fatty liver; FBS: fetal bovine serum; HCC: hepatocellular carcinoma; HGF: hepatocyte growth factor; HSCs: hepatic stellate cells; HSCFL: hepatic stellate cells isolated from fatty liver; HSCNL: hepatic stellate cells isolated from normal liver; HFD: high-fat diet; HIF: hypoxia inducible factor; IL-1α: interleukin-1α; IQGAP1: IQ motif containing GTPase activating protein 1; MMPs: matrix metalloproteinases; MTT: methyl thiazolyl tetrazolium; MAPK: mitogen-activated protein kinase; NAFLD: non-alcoholic fatty liver disease; NASH: non-alcoholic steatotic hepatitis; NL: normal liver; ROCK: Rho-associated kinase; SASP: senescence-associated secretory phenotype; SDF-1: stromal derived factor-1; TIMP-1: tissue inhibitor metalloproteinase-1; TGF-βRII: TGF-β receptor II; TGF-β: transforming growth factor-β; VEGF: vascular endothelial growth factor

Additional Supporting Information may be found in the online version of this article.

Brief description: Although fatty liver is associated with hepatocarcinogenesis, it is unclear whether fatty liver promotes hepatocellular carcinoma (HCC) progression. Through and in vivoimodels, we investigated whether steatotic liver promotes HCC progression and whether steatotic liver hepatic stellate cells (HSCs) are associated with HCC progression. Activated fatty liver HSCs significantly contributed to HCC proliferation and migration, and exhibited increased secretion of interleukin-α, vascular endothelial growth factor, and transforming growth factor-β in the tumor microenvironment.

Grant sponsor: Ministry of Education, Culture, Sports, Science and Technology; **Grant number:** 21591748

DOI: 10.1002/ijc.29096

History: Received 8 Dec 2013; Accepted 10 July 2014; Online 23 July 2014

Correspondence to: Hirotaka Tashiro, Department of Gastroenterological and Transplant Surgery, Applied Life Sciences, Institute of Biomedical & Health Sciences, Hiroshima University, 1-2-3, Kasumi, Hiroshima 734-8551, Japan, Tel.: +81-82-257-5222, Fax: +81-82-257-5224, E-mail: htashiro@hiroshima-u.ac.jp

What's new?

Fatty liver is associated with hepatocellular carcinoma (HCC), but its exact role has been unclear. In this study, the authors found that HCC metastasis was increased in rats whose livers were steatotic. They also found that when hepatic stellate cells (HSCs) from rats with steatotic livers were co-injected with HCC cells into normal rats, the resulting tumors were significantly larger than when normal HSC cells were used. The increased levels of cytokines secreted by activated fatty-liver HSCs may enhance proliferation and migration of HCC.

risk factors for the development of HCC,[3] and obesity is reported to be an independent risk factor for HCC recurrence after curative treatment, such as hepatectomy in patients with NASH.[4] It has been reported that obesity and fatty liver (FL) promote a chemical carcinogen-induced hepatocarcinogenesis.[5,6] However, the functional impact of FL on the progression and metastasis of HCC remains largely unexplored.

Hepatic stellate cells (HSCs) are key contributors to liver fibrosis and portal hypertension.[7–9] Recently, these cells were postulated to form a component of the pro-metastatic liver microenvironment because they can transdifferentiate into highly proliferative and motile myofibroblasts, which have been implicated in desmoplastic reactions and metastatic growth.[10,11] Moreover, HSC activation has been shown to correlate with the severity of hepatic steatosis.[12,13] Therefore, activated HSCs in FL may enhance the progression of HCC, but this possibility has not been fully explored. Therefore, we investigated whether FL in rats has a microenvironment that can promote the progression of HCC, and whether the HSCs in FL enhance the progression of HCC.

Material and Methods

Animals

Four-week-old male Buffalo and F344 nude rats were purchased from Clea Japan, (Tokyo, Japan), and F344 rats were purchased from Charles River Breeding Laboratories (Osaka, Japan). Four-week-old rats were fed a choline-deficient diet (CDD) (Oriental Yeast Co., Tokyo, Japan) for 6 weeks or a high-fat diet (HFD) for 16 weeks (F2HFD2, 82% kcal fat; Oriental Yeast Co.) to promote the development of FL. All animal experiments were performed according to the guidelines set by the United States National Institutes of Health (1996).

Cell lines

The rat HCC cell line McA-RH7777 was obtained from the American Type Culture Collection (Rockville, MD). The rat HCC cell lines C1 and L2 were kindly provided by Dr. K. Ogawa, National Institute of Health Sciences (Tokyo, Japan). The McA-RH7777 cell line originated in Buffalo rats, whereas the C1 and L2 cell lines originated in F344 rats. The cells were cultured in Dulbecco's modified Eagle's medium (DMEM) supplemented with 10% fetal bovine serum (FBS) in a humidified atmosphere of 5% CO_2 at 37°C.

Isolation of HSCs

HSCs were isolated from rat livers according to previously described procedures.[14] The purity of the cells was estimated through ordinal light and fluorescence microscopic examinations and by indirect enzyme immunoreactivity with an anti-desmin antibody (Dako, Versailles, France).

Conditioned medium

Conditioned medium (CM) was harvested from cultured HSCs after incubation in serum-free DMEM for 48 hr. At the end of the incubation period, the medium was stored at −80°C until use.

Proliferation assay

HCC cells were seeded at 5,000 cells per well in 96-well plates and cultured overnight in DMEM supplemented with 10% FBS. The medium was then changed to serum-free DMEM and CM. Incubations continued for 24 hr before the addition of 3-(4, 5-methylthiazol-2-yl)-2, 5-diphenyl-tetrazolium bromide [methyl thiazolyl tetrazolium (MTT), nonradioactive proliferation assay; Promega Corp, Madison, WI] for 4 hr. Cellular MTT was solubilized with acidic isopropanol, and the optical density was measured at 570 nm by using a 96-well plate reader. The survival fraction was then quantified.

Migration assay

For studies of HCC cell migration, 8-μm-pore size Transwell chambers (Corning, NY) were used. In total, 5×10^5 HSCs were seeded into the lower chamber that was coated with collagen type I in 1 mL of medium containing 10% FBS, and cultured for 48 hr. No HSCs were added to the control wells. The medium was changed to 750 μL of RPMI supplemented with 0.1% bovine serum albumin, and 2×10^4 HCC cells in 200 μL of RPMI with 0.1% bovine serum albumin were added to the upper chamber. After incubation at 37°C in 5% CO_2 for 24 hr, the non-migrating cells on the upper surface of the membrane were removed with a cotton swab. Cells were fixed in 4% paraformaldehyde and stained with propidium iodide solution (Dojindo, Kumamoto, Japan). Migrating cells were counted at 200× magnification in nine adjacent microscope fields for each membrane.

Enzyme-linked immunosorbent assay

The amount of vascular endothelial growth factor (VEGF), tissue inhibitor of metalloproteinases 1 (TIMP-1), matrix metalloproteinase-9 (MMP-9), transforming growth factor-β1 (TGF-β1), and interleukin 1α (IL-1α) were quantified using ELISA kits, according to the manufacturer's instructions (R&D Systems, Minneapolis, MN).

Western blot analysis

Cells were cultured in DMEM without 10% FBS overnight. Thereafter, the cells were incubated in the presence of CM for 10 min before being homogenized in lysis buffer (Cell Lysis Buffer; Cell Signaling Technology, Danvers, MA). Western blot analysis was performed as described previously.[14] Antibodies to β-actin were purchased from Abcam (Tokyo, Japan). Antibodies to Akt, p-Akt, anti-p44/42, mitogen-activated protein kinase (MAPK), and anti-phospho-p44/42 MAPK antibodies were purchased from Cell Signaling Technology (Beverly, MA). The phosphorylation levels were normalized to the levels of total Akt or MAPK protein expression.

Experimental model of intrahepatic HCC metastasis

HCC cells (5×10^6 cells or 5×10^5 cells/body) were implanted into the livers of rats *via* portal vein injection. In rats that were fed on a CDD, normal diets were given after the injection of the HCC cells, whereas in rats fed with a HFD, the HFD was continued until the study was completed. At the end of the experiment, rats were humanely sacrificed. The area of the liver occupied by tumor was calculated by averaging the percentage of the liver area occupied by tumor in microscopic sections continuously cut at 5-mm intervals.

Confocal immunofluorescence and histology

Phalloidin staining of isolated HSCs was performed as described previously.[14] Samples were observed under a conventional fluorescence microscope or a laser confocal microscope. For histological analysis, formalin-fixed liver tissue sections were cut, stained with hematoxylin–eosin, and examined microscopically. To assess the grade of the steatosis, sections were stained with oil red O.

HSC/tumor cell co-implantation model

C1 cells (5×10^6 cells/body) were implanted into the subcutis of F344 nude rats, either alone or in combination with HSCs isolated from F344 rats (5×10^6 cells/body). Successful implantation of HSCs was determined *via* frozen section analysis of the co-implantation of fluorescently labeled HSCs and HCC cells. The HSCs were fluorescently labeled with red fluorescent linker dye (PKH26 Red Fluorescent Cell Linker Kit; Sigma, Sigma-Aldrich, St Louis, MO) according to the manufacturer's instructions. At the end of the experiment, rats were humanely sacrificed. The largest tumor diameter and the tumor weight were measured 4 weeks after implantation. The survival of HSCs and cellular proliferation were assessed by immunohistochemical analysis of desmin and Ki-67 (BD Pharmingen, San Jose, CA), respectively.

Treatment of HSCs by Y-27632

The specific Rho-associated kinase (ROCK) inhibitor, Y-27632, was purchased from Wako (Osaka, Japan). Activated HSCs were deactivated by incubation with Y-27632 (10 μM) in serum-free DMEM for 3 hr.

Statistical analysis

The survival rates of rats were compared using the Kaplan–Meier method and were analyzed using the log-rank test. The tumor engraftment rates were compared by the chi-square test. One-way analysis of variance was used for multiple comparisons. All the data are expressed as the average (±SE). p Values less than 0.05 were considered statistically significant. Statistical analyses were performed with the SPSS software, version 16 (SPSS Japan, Tokyo, Japan).

Technical and material details of the cytokine assay are given in the Supporting Information Materials.

Results

CDD induced FL, activation of HSCs and increased secretion of cytokines

Feeding on a CDD for 6 weeks resulted in severe steatotic changes (60% macrosteatosis) (Supporting Information Fig. S1*a*). The purity of the isolated HSCs was estimated by fluorescence microscopic examination and by indirect enzyme immunoreactivity with an anti-desmin antibody, and was found to be >90% (Supporting Information Fig. S1*b*). HSCs isolated from FL (HSCFL) of rats fed on a CDD for 6 weeks had significantly increased stress fiber formation compared to HSCs isolated from normal liver (HSCNL) (Supporting Information Fig. S1*c*). We assessed the mediators secreted by cells in monoculture by performing cytokine arrays on CM samples. TIMP-1 and VEGF were detected in CM harvested from HSCFL, whereas they were not detected in CM harvested from HSCNL (Supporting Information Fig. S1*d*–S1*f*).

CDD-induced FL has a permissive microenvironment for HCC metastasis

To assess the effects of FL on HCC metastasis, we first implanted McA-RH7777 cells (5×10^5 cells/body) *via* the portal vein into the livers of syngeneic Buffalo rats. One of seven rats with normal livers (NLs) developed a small, single nodular HCC; all seven rats survived more than 8 weeks after inoculation of the HCC cells. In contrast, all ten rats with FL fed on a CDD for 6 weeks developed diffusely distributed tumors, and five of ten died of HCC within 8 weeks (Figs. 1*a*–1*c*). Volumes of the HCC tumors were significantly greater in rats with FL than in rats with NL (Fig. 1*d*).

In other experiments, L2 cells (5×10^6 cells/body) were injected into the portal veins of F344 rats that were fed on either a CDD or a normal diet. In all eight rats fed on a CDD for 6 weeks, multiple nodular liver tumors developed within 8 weeks, and four of these rats also developed pulmonary metastases. In contrast, none of the five rats fed on a normal diet developed tumors (Supporting Information Figs. S2*a* and S2*b*).

HSCFL stimulate HCC cell proliferation and migration *in vitro*

First, we investigated whether HSCFL could induce the proliferation of McA-RH7777 and C1 HCCs. When these cells were cultured with CM harvested from syngeneic HSCFL,

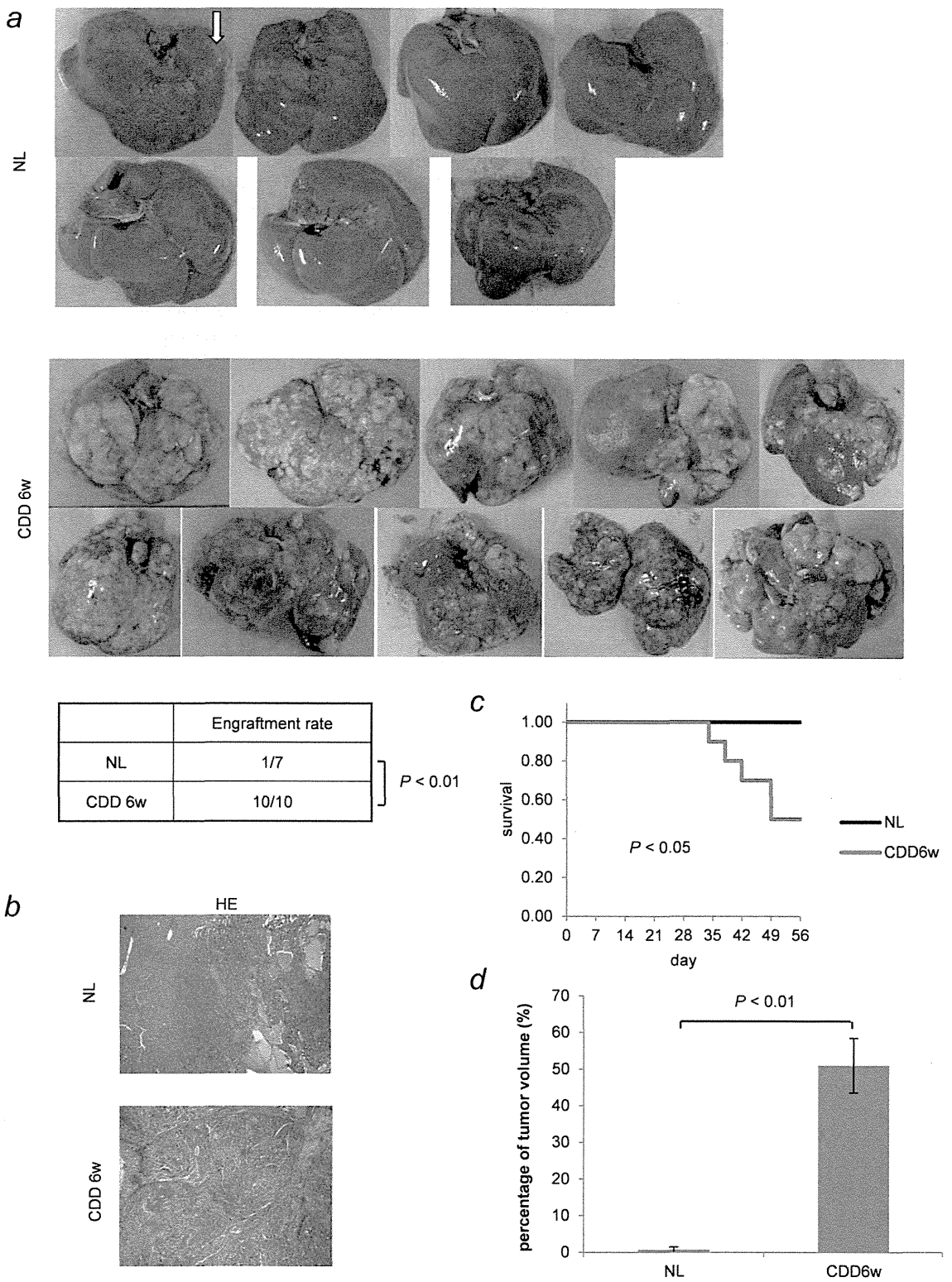

Figure 1. Choline deficient diet-induced FL has a permissive microenvironment for HCC metastasis. (*a*) Macrography of liver tumors in NL and FL. One of seven rats with NL developed a single nodular tumor (arrow) after inoculation of HCC cells (McA-RH7777 cells, 5×10^5 cells/body), whereas all ten rats with FL developed diffusely distributed liver tumors. (*b*) Hematoxylin-eosin-stained images of liver tumors in NL and FL. (*c*) Kaplan–Meier curve documenting the survival of rats inoculated with HCC cells. (*d*) The graph shows the percentage of tumor volume (tumor volume/liver volume). Results are presented as means (±SE).

their rate of proliferation increased, whereas when the cells were incubated with CM harvested from HSCNL, no increase in tumor cell proliferation occurred (Fig. 2*a*, Supporting Information Fig. S3*a*). We then examined whether HSCFL could induce migration of HCCs. HSCFL promoted HCC migration to a significantly greater extent than did HSCNL (Fig. 2*b*, Supporting Information Fig. S3*b*).

Factors secreted from HSCFL enhanced activation of MAPK and Akt pathways in HCC cells

To determine the signaling pathways that may be involved in the tumor-promoting effects of HSCFL, we examined McA-RH7777 cells treated with CM harvested from a monoculture of HSCFL for activation of Akt and MAPK by western blotting. The phosphorylation levels of Akt and ERK were significantly increased in cells treated with CM harvested from monoculture of HSCFL in comparison with CM harvested from HSCNL (Fig. 2*c*).

HCC-HSC cross-talk is bidirectional

We analyzed the secretion of VEGF, TGF-β1, IL-1α, MMP-9 and TIMP-1 by HCC cells and HSCs in monoculture and co-culture, using ELISA kits. Only an additive effect of VEGF and TGF-β1 was noted, and their levels were significantly increased in the CM harvested from co-culture of HCC cells and HSCFL compared with the levels in CM harvested from co-culture of HCC cells and HSCNL (Figs. 2*d* and 2*e*). Although HSCNL, HSCFL, and HCC cells barely secreted IL-1α and MMP-9, both factors were secreted in CM harvested from co-culture of HCC cells and HSCNL. Furthermore, the concentrations of IL-1α and MMP-9 were significantly increased in CM harvested from co-culture of HCC cells and HSCFL, due to a synergistic effect, compared to concentrations in CM harvested from co-culture of HCC cells and HSCNL (Figs. 2*f* and 2*g*). However, the concentration of TIMP-1 was significantly lower in CM harvested from co-culture of HCC cells and HSCFL compared to CM harvested from monoculture of HSCFL because of an inhibitory effect (Fig. 2*h*). These results suggested that cytokine secretions are altered through HCC-HSC interactions.

Co-implantation with HSCFL promotes HCC growth *in vivo*

We examined the effect of HSCFL on HCC growth *in vivo*. C1 cells, originating from F344 rat HCC cells, were implanted to the subcutis of syngeneic F344 nude rats, either alone or in combination with HSCFL or HSCNL from F344 rats. HSCNL and HSCFL were implanted to a similar extent, according to frozen section analysis, 2 days after the co-implantation of HSCs labeled by PKH26 and non-labeled HCC cells (Supporting Information Figs. S4*a* and S4*b*). When C1 cells (5×10^6 cells/body) were implanted into the subcutis of syngeneic F344 nude rats, three of the nine rats implanted with HCC cells alone and six of nine rats implanted with HCC cells and HSCNL developed tumors at the site of implantation, but all nine rats implanted with HCC cells and HSCFL developed tumors. Moreover, the rats implanted with HSCFL in addition to HCC cells developed significantly larger tumors than those implanted with HCC cells and HSCNL (Figs. 3*a*–3*d*). The presence of desmin-positive cells was determined by immunohistochemical analysis. The number of desmin-positive cells in the tumors of rats co-transplanted with HSCFL was comparable with those co-transplanted with HSCNL, whereas only a few desmin-positive cells were noted in tumors of rats implanted with C1 cells alone (Supporting Information Figs. S4*c* and S4*e*). In addition, we used immunohistochemistry to examine the expression of nuclear Ki-67, a cellular proliferation marker. The number of Ki-67-positive cells was significantly greater in the tumors of rats co-transplanted with HSCNL than in the tumors of rats transplanted with C1 cells alone. Furthermore, the number of Ki-67-positive cells was significantly increased in the tumors of rats co-transplanted with HSCFL compared with those co-transplanted with HSCNL (Supporting Information Figs. S4*d* and S4*f*).

Rho-kinase inhibitor attenuates HCC progression through deactivation of HSC-FL

We have previously shown that HSCFL exhibited increased stress-fiber formation and F-actin expression as compared to HSCNL,[14] and increased stress-fiber formation and F-actin expression in HSCFL were suppressed by treatment with the ROCK inhibitor, Y-27632. However, HSCFL were re-activated within 48 hr of Y-27632 administration (Fig. 4*a*). In this study, we investigated whether the ROCK inhibitor can deactivate activated HSCFL and suppress tumor progression in co-culture. First, we investigated the effect of Y-27632-treated HSCFL on the proliferation of McA-RH7777 cells by performing the MTT assay. When McA-RH7777 cells were cultured with CM harvested from Y-27632-treated HSCFL, cell proliferation was suppressed compared with that in CM harvested from untreated HSCFL (Fig. 4*b*). Thereafter, a migration assay showed that the migration of McA-RH7777 cells was significantly suppressed in co-culture with Y-27632-treated HSCFL compared with co-culture with untreated HSCFL (Fig. 4*c*). Furthermore, the enhancement in the proliferation and migration by Y-treated HSCFL were significantly greater than those of HSCNL (Figs. 4*b* and 4*c*). In addition, the phosphorylation levels of Akt and ERK were significantly decreased in HCC cells treated with CM harvested from monoculture of Y-27632-treated HSCFL compared with phosphorylation levels in HCC cells treated with CM harvested from untreated HSCFL (Fig. 4*d*). Moreover, an ELISA study showed that the levels of TGF-β1 were significantly lower in CM harvested from Y-27632-treated HSCFL than levels in CM harvested from untreated HSCFL (Fig. 4*e*). Moreover, the concentration of IL-1α was significantly decreased in CM harvested from a co-culture of HCC and HSCFL treated with Y-27632, compared to that in CM harvested from a co-culture of HCC and untreated HSCFL (Fig. 4*f*). However, the levels of VEGF and TIMP-1 in CM